METALLO - BIOACTIVE COMPOUNDS AS POTENTIAL NOVEL ANTICANCER THERAPY

Abdou S. El-Tabl[*1], Moshira M. Abd-El Wahed[2], Mohammed H. H. Abu-Setta[1]

[1]Department of Chemistry, Faculty of Science, El-Menoufia University,
Shebin El -Kom, Egypt.
[2]Department of Pathology, Faculty of Medicine, El-Menoufia University,
Shebin El-Kom, Egypt.

ABSTRACT

Mono and bi-organometallic complexes of Cu(II), Ni(II), Mn(II), Zn(II) and Ag(I) complexes with oxaloamide ligand has much potential as therapeutic and diagnostic agents. The ligand allows the thermodynamic and kinetic reactivity of the metal ion to be controlled and also provide a scaffold for functionalization. Specific examples involving the design of metal complexes as anticancer agents are discussed. These complexes have been synthesized and characterized by (1H-NMR, mass, IR, UV-VIS, ESR) spectra, magnetic moments and conductance measurements, elemental and thermal analyses. Molar conductances in DMF solution indicates that, the complexes are non-electrolytes. The ESR spectra of solid Cu(II) complexes (2-5) show an axial type indicating a d(X2-y2) ground state with a significant covalent bond character. However, Mn(II) complex(9), shows an isotropic type indicating an octahedral geometry. Cytotoxic evolution IC50 of the ligand and its complexes have been carried out. Cu(II) Complexes show enhanced activity in comparison to the parent ligand or standard drug. Copper is enriched in various human cancer tissues and is a co-factor essential for tumor angiogenesis processes. However, the use of copper binding ligand to target tumor, copper could provide a novel strategy for cancer selective treatment.

KEYWORDS

Complexes, Synthesis, Schiff Base, ESR, Cytotoxicity.

1. INTRODUCTION

Schiff bases have played a key role in the development of coordination chemistry. Schiff- base compounds containing an imine group are usually formed by the condensation of a primary amines with an active carbonyl or aldehyde group. These compounds are considered as a very important class of organic compounds, which have wide applications in many biological aspects [1].Various Schiff–bases complexes were reported to possess geno-toxicity [2,3],antibacterial [4,5] and antifungal activities [6]. The increasing interest in transition metal complexes containing Schiff-base ligand is derived from their well-established role in biological systems as well as their catalytic and pharmaceutical application [7]. Metal complexes provide a highly versatile platform for drug design. Besides variation in the metal and its oxidation state, that allow the fine-tuning of their chemical reactivity in terms of both kinetics and thermodynamics. Not only the metal but also the ligands can play important roles in biological activity, ranging from outer-sphere recognition of the target site to the activity of any released ligands and ligand

DOI: 10.5121/ijac.2018.4102

centered redox processes. Due to a growing interest in the in the development of metallo-therapeutic drugs and metal-based agents [8,9], we reported herein synthesis and characterization of new metallo-therapeutic candidates derived from the novel ligand N^1,N^2-bis(2-((Z)-(2-hydroxylbenzylidene) amino)phenyl)oxalamide The cytotoxic activity of synthesized compounds has been also investigated.

2. MATERIALS AND METHODS

All the reagents employed for the preparation of the ligand and its complexes were synthetic grade and used without further purification. TLC is used to confirm the purity of the compounds. C, H, N and Cl analyses were determined at the Analytical Unit of Cairo University, Egypt. A standard gravimetric method was used to determine metal ions [10,12]. All metal complexes were dried under vacuum over P_4O_{10}. The IR spectra were measured as KBr pellets using a Perkin-Elmer 683 spectrophotometer (4000-400 cm^{-1}). Electronic spectra (qualitative) were recorded on a Perkin-Elmer 550 spectrophotometer. The conductance(10^{-3}M) of the complexes in DMF were measured at 25°C with a Bibby conduct meter type MCl. ^{1}H-NMR spectra of the ligand and its Zn(II) complex**(7)** were obtained with Perkin-Elmer R32-90-MHz spectrophotometer using TMS as internal standard. Mass spectra were recorded using JEULJMS-AX-500 mass spectrometer provided with data sys-tem. The thermal analyses (DTA and TGA) were carried out in air on a Shimadzu DT-30 thermal analyzer from 27 to 800°C at a heating rate of 10°C per minute. Magnetic susceptibilities were measured at 25°C by the Gouy method using mercuric tetrathiocyanatocobalt(II) as the magnetic susceptibility standard. Diamagnetic corrections were estimated from Pascal's constant [13]. The magnetic moments were calculated from the equation:

$$(\mu_{eff} = 2.828\ (X_n \times T)^{1/2}) \quad (1)$$

The ESR spectra of solid complexes at room temperature were recorded using a varian E-109 spectrophotometer, DPPH was used as a standard material. The TLC of all compounds confirmed their purity.

Preparation of the ligand

Preparation of N^1,N^2-bis(2-aminophenyl)oxalamide:N^1,N^2-bis(2-aminophenyl)oxalamide (Scheme 1) was prepared by adding equimolar amount of diethyl oxalate (15.70 g, 1 mol), to benzene-1,2diamine (23.24 g, 2 mol) in 50 cm^3 of absolute ethanol. The mixture was refluxed with stirring on water bath for 2hours and then left to cool at room temperature, filtered off, washed with water, dried and recrystallized from ethanol to afford N^1,N^2-bis(2-aminophenyl)oxalamide.

Preparation of the Schiff-base ligand N^1,N^2-bis(2-((Z)-(2-hydroxybenzylidene) amino) phenyl) oxalamide (HL): The ligand [HL] N^1,N^2-bis(2-((Z)- (2-hydroxybenzylidene) amino) phenyl)oxalamide (Scheme 1) was prepared by adding equimolar amount of N^1,N^2-bis(2-aminophenyl)oxalamide (22.40 g, 1 mol) to salicyaldehyde (32.3 g, 2 mol) in 50 cm^3 of absolute ethanol. The mixture was refluxed with stirring on water bath for 2 hours and then left to cool at room temperature, filtered off, washed with water, dried and recrystallized from ethanol to afford ligand (**1**). Ligand (1): Yield 91 %; m.p. 290; color is cumin green; Anal. Calcd. (%)for `$C_{28}H_{22}N_4O_4$ (FW = 478.50): C, 70.28; H, 4.63; N, 11.71; Found (%) C, 69.63; H, 5.08; N, 11.16; IR (KBr, cm^{-1}), 3450, υ(OH), 3260m, υ(NH), 1622 υ(C=N), 1477, 758 $\upsilon(C{=}C)_{Ar}$, 1615 $\upsilon(C{=}C)_{Al}$, 1324 υ(C-OH) , 1040 υ(N-N); ^{1}H-NMR [DMSO-d_6]: 10 (s, 1H, ^{26}O*H*); 8.8 (s, 1H,

NH[7]); 8.7 (s, 1H, NH[11]); 8.40 (s, 1H, [19]H-C=N); 9.1 (s, 1H, NH[10]); 3.4 (s, 1H, H[8]); 6.04-7.8 (m, 10 H, aromatic protons).

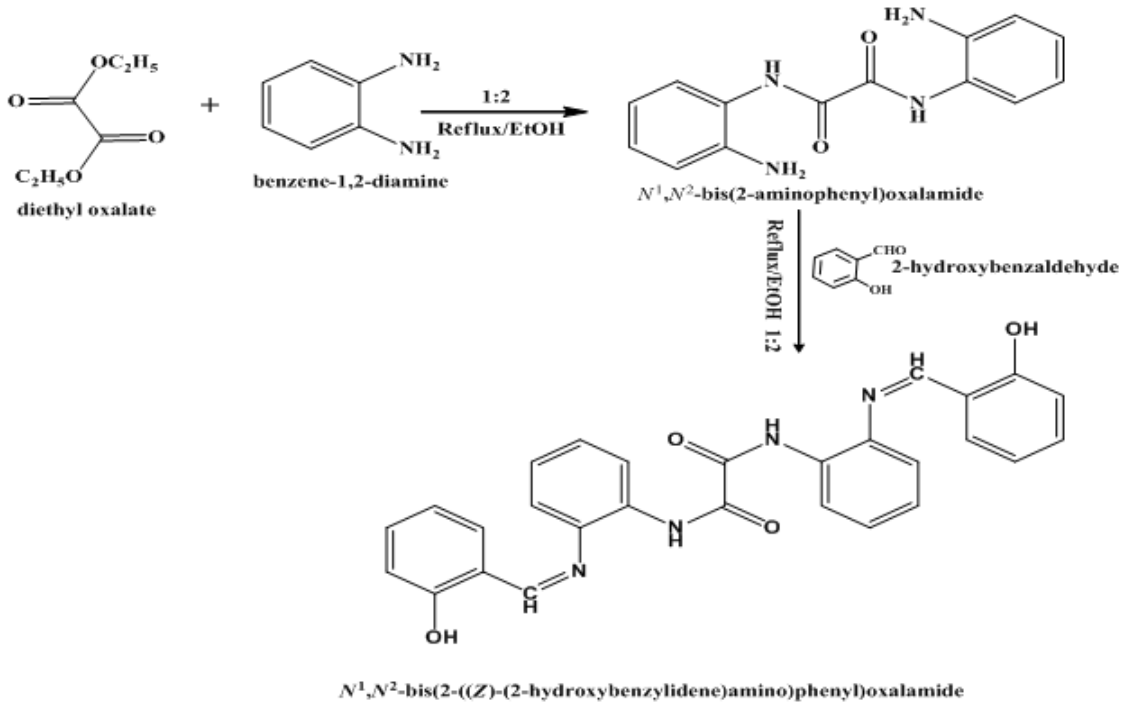

Scheme 1: Preparation of Ligand, N1,N2-bis(2-((Z)-(2-hydroxybenzylidene)amino)phenyl)oxalamide

Synthesis of metal complexes (2)-(10): The metal complexes **2, 4-7, 9 and 10** were prepared by refluxing with string a suitable amount (1 mmol) of a hot ethanolic solution of the following metal salts: $Cu(CH_3COO)_2.H_2O$, $CuCl_2{\cdot}2H_2O$, $Mn(CH_3COO)_2{\cdot}4H_2O$, $Zn(CH_3COO)_2{\cdot}2H_2O$ and $Ag(CH_3COO)$
(1 mmol) with a hot ethanolic solution of the ligand (4.0 g 1 mmol, 40 mL ethanol). The same method is used to prepare complex **3**but in molar ratio (1 metal: 2 ligand) using the following metal salt: $Cu(CH_3COO)_2.H_2O$and also mixed metal salts complex **8** ($Cu(CH_3COO)_2.H_2O$and $Zn(CH_3COO)_2{\cdot}2H_2O$) but in molar ratio (1 metal: 1 metal: 1 ligand).The refluxing times varied from 2 to 4 hours according to the depending to nature of metal ion, which led to precipitate of metal complexes. The precipitates, were filtered off, washed with ethanol then by diethyl ether and dried in vacuum desiccators over P_4O_{10}. Analytical data for the prepared complexes are:

Complex (2),$[(HL)Cu(CH_3COO)(H_2O)_2]$**:** Yield: 79 %; m.p. >300 ^oC; color: green; molar conductivity (Λ_m): 7.9$ohm^{-1}cm^2mol^{-1}$.Anal.Calcd. (%)for$C_{30}H_{28}N_4O_8Cu$ (FW = 636.11): C, 56.64; H, 4.44; N, 8.81,

Cu, 9.99; Found (%) C, 56.77; H, 4.45; N, 8.9, Cu, 10.00; IR (KBr, cm^{-1}), 3420, υ(OH), 3054υ(NH), 1680υ(C=N), 1714, 1680υ(C=O), 1321υ(C-O), 590υ(M←O), 442υ(M←N), 1557, 1343$\upsilon_{sym}CH_3COO$, $\upsilon_{asym}CH_3COO$ (Δ=214 cm^{-1}).

Complex (3) $[(L)Cu(CH_3COO)(H_2O)_2]_2$**:** Yield: 85 %; m.p. >300 ^oC; color: green; molar conductivity (Λ_m): 7.4$ohm^{-1}cm^2mol^{-1}$.Anal.Calcd. (%)for$C_{32}H_{34}N_4O_{12}Cu_2$ (FW = 793.08): C, 48.42; H, 4.32; N, 7.06, Cu, 16.01; Found (%) C, 48.7; H, 4.4; N, 7.1, Cu, 16.1; IR (KBr, cm^{-1}), 3405, υ(OH), 3058υ(NH), 1600,1549υ(C=N), 1671 υ(C=O), 1322 υ(C-O), 648υ(M←O), 501υ(M←N), 1430,1260,1389,1251$\upsilon_{sym}CH_3COO$, $\upsilon_{asym}CH_3COO$ (Δ=170cm^{-1} and 138 cm^{-1} respectively).

Complex (4),$[(HL)(Cu)Cl(H_2O)_2]$**:** Yield: 80 %; m.p.>300^oC; color: brown; molar conductivity (Λ_m): 9.2$ohm^{-1}cm^2mol^{-1}$.Anal.Calcd. (%)for$C_{28}H_{25}N_4O_6ClCu$ (FW = 612.52): C, 54.90; H, 4.11; N, 9.15, Cu, 10.37; Found (%) C, 55.00; H, 4.2; N, 9.3, Cu, 10.4; IR (KBr, cm^{-1}), 3435υ(OH), 3165υ(NH), 1610 υ(C=N), 1690, 1681υ(C=O), 1310 υ(C-O), 639υ(M←O), 504υ(M←N), 467υ(M-Cl).

Complex (5),$[(H_2L)Cu(SO_4)(H_2O)_2].2H_2O$**:** Yield: 79 %; m.p. >300^oC; color: brown; molar conductivity (Λ_m): 9.2$ohm^{-1}cm^2mol^{-1}$. Anal.Calcd. (%)for$C_{28}H_{29}N_4O_{12}SCu$ (FW = 710.17): C, 47.35; H, 4.26; N, 7.89, Cu, 8.95; Found (%) C, 47.4; H, 4.3; N, 7.8, Cu, 8.8; IR (KBr, cm^{-1}), 3440 υ(OH), 3070υ(NH), 1611υ(C=N), 1690,1681υ(C=O), 1304 υ(C-O), 616υ(M←O), 503υ(M←N),1170,1118,1056,725 υ(SO_4).

Complex (6),$[(HL)Zn(CH_3COO)(H_2O)_2]$**:** Yield: 85 %; m.p. >300^oC; color: yellow; molar conductivity (Λ_m): 7.9$ohm^{-1}cm^2mol^{-1}$. ForAnal. Calcd. (%)for$C_{30}H_{28}N_4O_8Zn$ (FW = 637.95): C, 56.48; H, 4.42; N, 8.78Zn, 10.25; Found (%) C, 56.5; H, 4.4; N, 8.9, Zn, 10.3; IR (KBr, cm^{-1}), 3395 υ(OH), 3052υ(NH), 1626υ(C=N), 1691,1680 υ(C=O), 1248 υ(C-O), 639υ(M←O), 534υ(M←N), 1421,1321,$\upsilon_{sym}CH_3COO$, $\upsilon_{asym}CH_3COO$ (Δ=100 cm^{-1}).

Complex (7),$[(H_2L)Zn(SO_4)(H_2O)_2]$**:** Yield: 78 %; m.p. >300^oC; color: green; molar conductivity (Λ_m): 6.9$ohm^{-1}cm^2mol^{-1}$.Anal.Calcd. (%)for$C_{28}H_{25}N_4O_{10}SZn$ (FW = 675.97): C, 49.75; H, 3.88; N, 8.29, Zn, 9.67; Found (%) C, 49.68; H, 3.89; N, 8.20, Zn, 9.58; IR (KBr, cm^{-1}), 3415 υ(OH), 3051 υ(NH), 1605 υ(C=N), 1714,1681υ(C=O), 1304 υ(C-O), 585υ(M←O), 471 υ(M←N), 1157,1098,1040,1030, 750υ(SO_4).

Complex (8),$[(L)CuZn(CH_3COO)_2(H_2O)_4]$**:** Yield: 75 %; m.p.>300 ^oC; color: green; molar conductivity (Λ_m): 9.9$ohm^{-1}cm^2mol^{-1}$.Anal.Calcd. (%)for$C_{32}H_{34}N_4O_{12}CuZn$ (FW = 795.56): C, 48.31; H, 4.31; N, 7.04, Cu, 7.99; Zn, 8.22; Found (%) C, 48.4; H, 4.2; N, 7.01, Cu, 7.97; Zn, 8.20; IR (KBr, cm^{-1}), 3413 υ(OH), 3053 υ(NH), 1605υ(C=N), 1681,1679 υ(C=O), 1320 υ(C-O), 749υ(M←O), 640υ(M←N), 1477, 1372, 1430, 1320$\upsilon_{sym}CH_3COO$, $\upsilon_{asym}CH_3COO$ (Δ=105 cm^{-1} and 110 cm^{-1} respectively).

Complex (9),$[(HL)Mn(CH_3COO)(H_2O)_2]$**:** Yield: 67 %; m.p. >300 ^oC; color: yellow; molar conductivity (Λ_m): 9.7$ohm^{-1}cm^2mol^{-1}$.Anal.Calcd. (%)for$C_{30}H_{28}N_4O_8Mn$ (FW = 627.50): C, 57.42; H, 4.50; N, 8.93, Mn, 8.76; Found (%) C, 57.9; H, 4.30; N, 8.95, Mn, 8.77; IR (KBr, cm^{-1}), 3377 υ(OH), 3049 υ(NH), 1602 υ(C=N), 1689,1681 υ(C=O), 1107 υ(C-O), 582υ(M←O), 497υ(M←N), 1465, 1352$\upsilon_{sym}CH_3COO$, $\upsilon_{asym}CH_3COO$ (Δ=113cm^{-1}).

Complex (10),$[(H_2L)Ag(CH_3COO)]$**:** Yield: 69%; m.p.>300 ^oC; color: yellow; molar conductivity (Λ_m): 9.8$ohm^{-1}cm^2mol^{-1}$.Anal.Calcd. (%)for$C_{30}H_{25}N_4O_6Ag$ (FW = 645.41): C, 55.83; H, 3.90; N, 8.68, Ag, 16.71; Found (%) C, 55.87; H, 3.79; N, 8.69, Ag, 16.72; IR (KBr, cm^{-1}),

3409 υ(OH), 3053υ(NH), 1610 υ(C=N), 1700,1680 υ(C=O), 1247 υ(C-O), 529υ(M←O), 469υ(M←N), 1500, 1380$\upsilon_{sym}CH_3COO$, $\upsilon_{asym}CH_3COO$ (Δ=120 cm^{-1}).

3. BIOLOGICAL ACTIVITY

Cytotoxic activity: Evaluation of the cytotoxic activity of the ligand and its metal complexes was carried out in the Pathology Laboratory, Pathology Department, Faculty of Medicine, El-Menoufia University, Egypt. The evaluation process was carried out in vitro using the Sulfo-Rhodamine-B-stain (SRB) assay published method [14,15]. Cells were plated in 96-multiwell plate (10^4cells/well) for 24 hrs. Before treatment with the complexes to allow attachment of cell to the wall of the plate. Different concentrations of the compounds under test in DMSO (0, 5, 12.5, 25 and 50 µg/ml) were added to the cell monolayer, triplicate wells being prepared for each individual dose. Monolayer cells were incubated with the complexes for 48 hrs.at 37°C and under 5% CO_2. After 48 hrs. cells were fixed, washed and stained with Sulfo-Rhodamine-B-stain. Excess stain was wash with acetic acid and attached stain was recovered with Tris EDTA buffer. Color intensity was measured in an ELISA reader. The relation between surviving fraction and drug concentration is plotted to get the survival curve for each tumor cell line after addition the specified compound.

4. RESULTS AND DISCUSSION

All the metal complexes are stable at room temperature, non hydroscopic, insoluble in water, partially soluble in MeOH, EtOH, $CHCl_3$ and $(CH_3)_2CO$ and completely soluble in DMF and DMSO. The analytical and physical data, spectral data (experimental part, Tables 1-2) are compatible with the proposed structures, Figure 1-4. The molar conductance of the complexes in 10^{-3} M DMF at 25 ^oC are in the 10.12-4.72 $ohm^{-1}cm^2mol^{-1}$ range, indicating a non-electrolytic nature [19]. These low values commensurate the absence of any counter ions in their structure [17]. Many attempts were made to grow a single crystal but unfortunately, they were failed. Reaction of the ligand **(1)** with metal salts using (1L: 1M), (1L: 2M) and (1L: 1M: 1M*), molar ratios in ethanol gives complexes **(2)-(10)**.

Proton Nuclear Magnetic Resonance spectra (^{1}H-NMR)of the ligand (1) and Zn(II) complex (7): The ^{1}H-NMR spectra of ligandand Zn(II) complex **(7)** in deutrated DMSO show peaks consistent with the proposed structure. The ^{1}H-NMR spectrum of the ligand shows chemical shift observed as singlet at 11.9 ppm (s, 2H, O$H^{27,35}$) which is assigned to proton of aromatic hydroxyl group. The chemical shifts which appeared at 8.0-8.1ppm range is attributed tothe azomethine protons ($^{12.20}$H-C=N). However, the chemical shifts appeared as a singlet at 5.4 ppm is attributed to the proton of NH attached to carbonyl group. A set of signals appeared as multiples in the 6.4-7.5 ppm range, corresponding to protons of aromatic ring [21]. By comparison the ^{1}H NMR of the ligand and the spectrum of the Zn(II) complex **(7)**. The absence of the signal characteristic to the O*H* group indicating that the ligand bonded with the Zn(II) ions in its deprotonated form. In addition, there is a significant downfield shift of the azomethine proton signal and one from NH groups attached to carbonyl group relative to the free ligand clarified that the metal ions are coordinated to the azomethine nitrogen atom and NH nitrogen atom. This shift may be due to the formation of a coordination bond (N→M) [19,17].

Mass spectra: The mass spectra of(**1**) and its, Cu(II) complexes, (**2**),(**4**),**(5)**Zn(II) complex **(7)**and mixed complex (**8**) confirmed their proposed formulation. The spectrum of (**1**)reveals the molecular ion peak (m ⁄z) at 478.5 amu consistent with the molecular weight of the ligand. Furthermore, the fragments observed at (m⁄z) = 55, 79, 106, 210, 367 and 478.5 amu correspond to C_4H_7, C_6H_7, C_8H_{10}, $C_{16}H_{18}$, $C_{27}H_{15}N_2$ and $C_{28}H_{22}N_4O_4$ moieties respectively. Complex (**2**) shows fragments (m⁄z) at 55, 91, 210, 316 and 636 amu due to C_4H_7, C_7H_7, $C_{16}H_{18}$, $C_{22}H_{10}N_3$ and $C_{30}H_{28}CuN_4O_8$ moieties respectively. The fragments observed (m⁄z) at 80, 147, 334, 458 and 612 amu for complex(**4**) were assigned to $C_2H_{12}N_2O$, $C_4H_{11}N_4O_2$, $C_{16}H_{22}N_4O_4$, $C_{24}H_{36}N_5O_4$ and $C_{28}H_{25}ClCuN_4O_6$moieties, whereas the spectrum of Cu(II) complex (5) showed molecular ion peak at 673 assigned to the molecular weight of the complex and also showed fragments at 78, 91,106, 181, 210 and316 which were assigned to C_6H_6,C_7H_7, C_8H_{10},$C_{14}H_{13}$, $C_{16}H_{18}$ and $C_{22}H_{10}N_3$. However, Zn(II) complex (**7**)gave fragments (m⁄z) at 121, 223, 388 and 676 amu , corresponding to $C_3H_{11}N_3O_2$, $C_9H_{11}N_4O_3$, $C_{20}H_{28}N_4O_4$ and $C_{28}H_{26}ZnN_4O_{10}S$ moieties respectively. Mixed complex(**8**) showed fragments (m⁄z) at 119, 197, 257, 484, 590 and 795.5 amu due to $C_3H_9N_3O_2$, $C_7H_9N_4O_3$, $C_{11}H_{21}N_4O_3$, $C_{27}H_{26}N_5O_4$, $C_{31}H_{42}N_8O_4$ and $C_{32}H_{34}CuZnN_4O_{12}$moieties respectively.

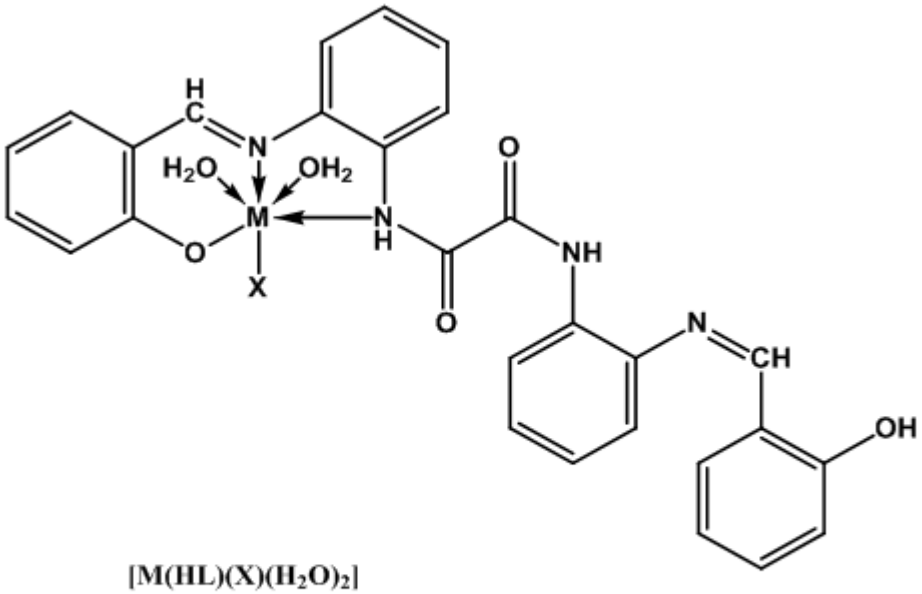

[M(HL)(X)(H$_2$O)$_2$]

M= Cu(II), X= OAc	**(2)**
M= Cu(II), X= Cl	**(4)**
M= Zn(II), X= OAc	**(6)**
M= Mn(II), X= OAc	**(9)**

Fig. 1: Structure representation of Cu(II), Zn(II), Mn(II) complexes (2, 4, 6and 9)

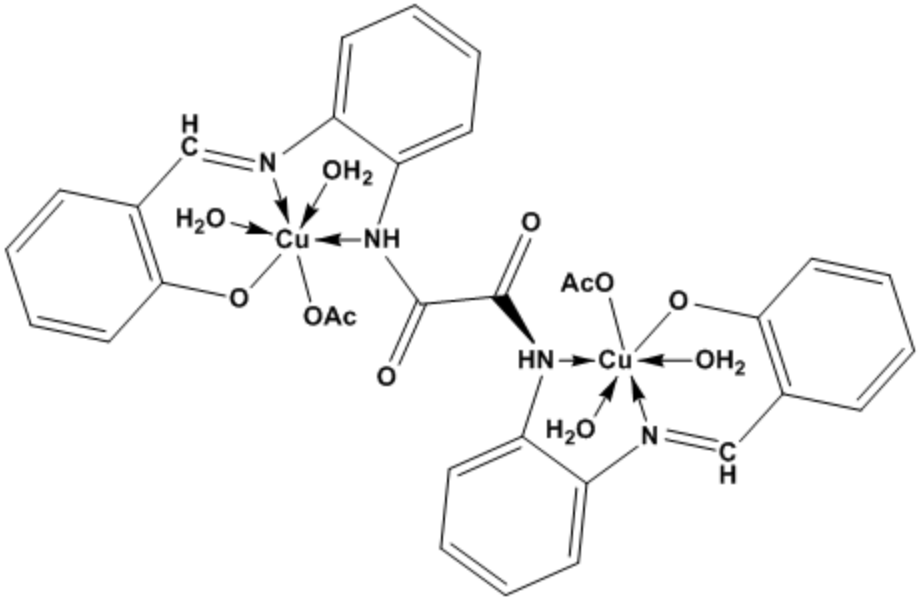

Fig. 2: Structure representation of Cu(II) complex**(3)**

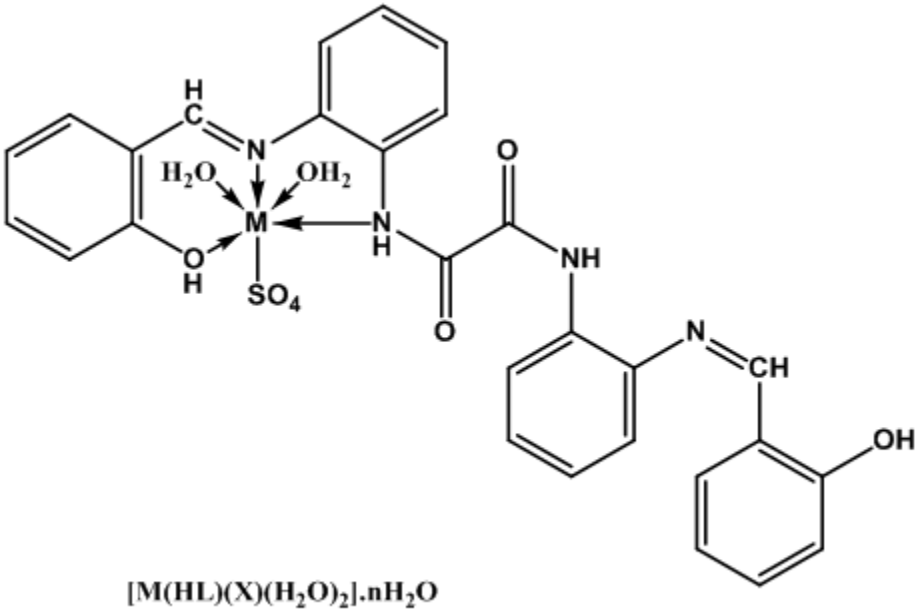

[M(HL)(X)(H$_2$O)$_2$].nH$_2$O
M= Cu(II), n= 2 (5)
M= Zn(II), n= 0 (7)

Fig.3: Structure representation of Cu(II), Zn(II) complexes**(5)** and **(7)**

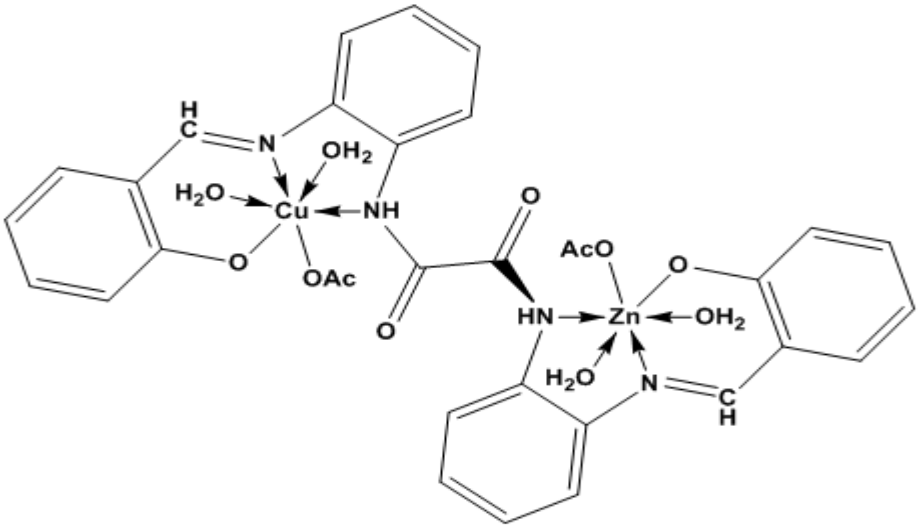

Fig.4: Structure representation of Cu(II) and Zn(II) mixed complex**(8)**

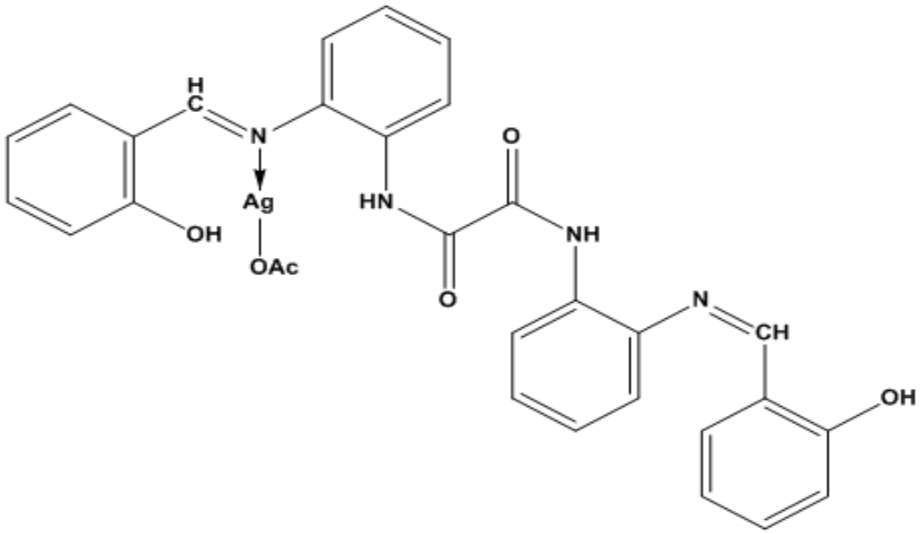

Fig.5: Structure representation of Ag(I) complex (10)

Infrared spectra (IR): The mode of bonding between the ligand and the metal ion revealed by comparing the IR spectra of the ligand (**1**) and its metal complexes (**2**)-(**10**). The ligand shows bands in the 3620-3230 and 3220-2500 cm^{-1} ranges, commensurate the presence of two types of intra- and intermolecular hydrogen bonds of OH and NH groups with imine group [24]. Thus, the higher frequency band is associated with a weaker hydrogen bond. The medium band at 3260 cm^{-1} is assigned to v(NH) groups [24,25]. The v(NH) group in the complexes appears shifted from the region of the free ligand indicating that, the NH group is involved in the coordination to the metal ion [26]. However, the characteristic bands of imines, v(C═N) and v(CH═C) were observed at 1623 and 1615 cm^{-1} respectively. Strong band appears at 1393cm^{-1} is attributed to the v(C-OH) vibration. The bands appear at 1490 and 762 cm^{-1} range, are assigned to v(Ar) vibration [26,27]. By comparing the IR spectra of the complexes (**2**)-(**10**) with that of the free ligand. It was

found that, the position of the v(C═N) bands of imines is shifted by 21-74 cm^{-1} range towards lower wave number in the complexes indicating coordination through nitrogen of azomethine group (CH═N) [26,27]. This is also confirmed by the appearance of new bands in the 640-442 cm^{-1} range, this has been assigned to the v(M-N) [27]. Complexes (**2**)-(**4**), (**6**), (**8**) and (**9**)show v(C-O) band in the 1322-1107 cm^{-1} range, indicating deprotonated of (C-OH) and lowering the value of the group confirming coordinated to the metal ion, However, complexes (**5**), (**7**) and (**10**) show v(C-OH) in the 1304-1247 range, indicating coordination to the metal ion [28]. The aromatic ring to the metal ion appears in the 1480-1455 cm^{-1} and 754-747 cm^{-1} ranges [30]. The IR spectra of the metal complexes (**2**)-(**10**) show bands in the 3635-3520 cm^{-1}, 3700-3200 cm^{-1}, 3280-3210 cm^{-1} and 2760-2470 cm^{-1} ranges, commensurate the presence of two types of intra-and intermolecular hydrogen bonds. In acetate complexes, the acetate ion may be coordinate to the metal ion in unidentate manner [29]. In the case of acetate complexes (**2**), (**3**), (**6**), (**8**), (**9**) and (**10**) show bands in the 1260-1557 and 1251-1443 cm^{-1} ranges, assigned to the asymmetric and symmetric stretches of the COO group. The mode of coordination of acetate group has often been deduced from the magnitude of the observed separation between the $\upsilon_{asym.}(COO^-)$ and $\upsilon_{sym.}(COO^-)$. The separation value (Δ) between $\upsilon_{asym}(COO^-)$ and $\upsilon_{sym.}(COO^-)$ in this complex was in the 105-214 cm^{-1} range suggesting the coordination of acetate group in these complexes as a monodentate fashion [24,29]. The sulphato complex (**5**) showsbands at 1170, 1118, 1056 and 725 cm^{-1}, and complex **(7)** shows bands at 1157, 1098, 1040, 1030 and 750 cm^{-1}which assigned to monodentatesulphate group [30]. Complexes (**2**)-(**10**) show bands in the 640-442 cm^{-1} is assigned to v(M-N) [29]. Complexes (**2**)-(**10**) show bands in the 749-529 cm^{-1} are due to v(M-O) [28].

Magnetic moments: The magnetic moments of the metal complexes (**2**)-(**10**) at room temperatures are shown in (Table 1). Copper(II) complexes (**2**)-(**5**) show values in the 1.5-1.7B.M, range corresponding to one unpaired electron in an octahedral structure [17,32]. Manganese(II) complex (**9**) show value 5.7, indicating high spin octahedral geometry around the Mn(II) ion [24,34]. Zn(II) complexes (**6**) and (**7**) and Ag(I) Complex **(10)**show diamagnetic property [35]. Mixed complex (**8**) shows value 1.76 B.M, indicating an octahedral complex[36].

Electronic spectra: The electronic spectral data for the ligand (**1**) and its metal complexes in DMF solution are summarized in (Table 1). Ligand (**1**) in DMF solution shows two bands at 320 nm (ε =7.72 x 10^{-3} mol^{-1} cm^{-1}) and 295 nm (ε = 7.12x 10^{-3} mol^{-1} cm^{-1}) which may be assigned to $n\rightarrow\pi^*$ and $\pi\rightarrow\pi^*$ transitions of the immine and aromatic ring respectively [33]. Copper(II) complexes (**2**), (**3**), (**4**) and (**5**) show bands in the 295-275 and 310-305 nm ranges , these bands are due to intraligand transitions, however, the bands appear in the 495-450, 580-500 and 620-600 nm ranges, are assigned to O→Cu, charge transfer, $^2B^1\rightarrow{}^2E$ and $^2B_1\rightarrow{}^2B_2$ transitions, indicating a distorted tetragonal octahedral structure [37,38]. However, manganese(II) complex (**9**) show bands in the 288-285, 340-300, 440-400, 585-510 and 623-620 nm, the first two bands are within the ligand, however, the other bands are corresponding to $^6A_{1g}\rightarrow{}^4E_g$, $^6A_{1g}\rightarrow{}^4T_{2g}$ and $^6A_{1g}\rightarrow{}^4T_{1g}$ transitions which are compatible to an octahedral geometry around the Mn(II) ion [42]. Zinc(II) complexes (**6**) and **(7)**, mixed complex (**8**), and silver(I) complex **(10)** show bands due to intraligand transitions [42].

Electron spin resonance (ESR): The ESR spectral data for complexes **(2)-(4)** and **(9)** are presented in (Table2a). The spectra of copper(II) complexes (**2-4**) are characteristic of species d^9 configuration having axial type of a $d_{(x2-y2)}$ ground state which is the most common for copper(II) complexes [25,29]. The complexes show $g_{\|}>g_{\perp}>2.0023$, indicating octahedral geometry around copper(II) ion [45,46].The g-values are related by the expression $G = (g_{\|}-2)/ (g_{\perp} -2)$ [45,47],

where (G) exchange coupling interaction parameter (G). If G<4.0, a significant exchange coupling is present, whereas if G value > 4.0, local tetragonal axes are aligned parallel or only slightly misaligned. Complexes**(2)**, (**3**) and (**4**) show 3.28, 2.85 and 3.37 values indicating spin-exchange interactions take place between copper(II) ions. This phenomena is further confirmed by the magnetic moments values in the (1.65– 1.7 B.M.) range. The $g_{\|}/A_{\|}$ value is also considered as a diagnostic term for stereochemistry [48], the $g_{\|}/A_{\|}$ values in the (105-135 cm^{-1}) range are expected for copper complexes within perfectly square planar geometry and for tetragonal distorted octahedral complexes are 150-250 cm^{-1}. The $g_{\|}/A_{\|}$ values for the copper complexes are lie just within the range expected for the tetragonal distorted octahedral copper(II)complexes (Table2a). The g-value of the copper(II) complexes with a $^2B_{1g}$ ground state ($g_{\|}>g_{\perp}$) may be expressed by [49]:

$$g_{\|} = 2.002 - (8K^2_{\|}\lambda^{\circ}/\Delta E_{xy}) \quad (2)$$

$$g_{\perp} = 2.002 - (2K^2_{\perp}\lambda^{\circ}/\Delta E_{xz}) \quad (3)$$

Where $k_{\|}$ and $k_{\perp}$ are the parallel and perpendicular components respectively of the orbital reduction factor (K), λ° is the spin-orbit coupling constant for the free copper, ΔE_{xy} and ΔE_{xz} are the electron transition energies of $^2B_{1g}\rightarrow{}^2B_{2g}$ and $^2B_{1g}\rightarrow{}^2E_g$. From the above relations, the orbital reduction factors ($K_{\|}$, $K_{\perp}$, K), which are measure terms for covalency [58], can be calculated. For an ionic environment, K=1; while for a covalent environment, K<1. The lower the value of K, the greater is the covalency.

Table 1: Electronic Spectra (nm) and magnetic moments (B.M) for the Ligand and Its Complexes

No.	Ligand/Complexes	λ_{max} (nm)	μ_{eff} (BM)	ν_2/ν_1
(1)	$[H_2L]$	295 nm (ε = 7.12x 10^{-3} mol^{-1} cm^{-1}) 320 nm (ε= 7.72 x 10^{-3} mol^{-1} cm^{-1})	-	-
(2)	$[(HL)Cu(CH_3COO)(H_2O)_2]$	290,310,495,540,600	1.70	-
(3)	$[(L)Cu(CH_3COO)(H_2O)_2]_2$	295,305,465,560,615	1.65	-
(4)	$[(HL)(Cu)Cl(H_2O)_2]$	285,293,310,465,580,610	1.69	-
(5)	$[(H_2L)Cu(SO_4)(H_2O)_2].2H_2O$	275,305,450,500,600,620	1.72	-
(6)	$[(HL)Zn(CH_3COO)(H_2O)_2]$	290,300,455,565,615	Dia.	-
(7)	$[(H_2L)Zn(SO_4)(H_2O)_2]$	287,315,350, 390,450,520,580,650	Dia.	-
(8)	$[(L)CuZn(CH_3COO)_2(H_2O)_4]$	285,320,350,390,450,625	1.76	--
(9)	$[(HL)Mn(CH_3COO)(H_2O)_2]$	285,300,340,400, 440,510,585,620, 623	5.83	-
(10)	$[(H_2L)Ag(CH_3COO)]$	285,288,305,330,420,620	Dia.	-

$$K^2_{\perp} = (g_{\perp} - 2.002)\ \Delta E_{xz}\ /2\lambda_o \quad (4)$$

$$K^2_{\|} = (g_{\|} - 2.002)\ \Delta E_{xy}\ /8\lambda_o \quad (5)$$

$$K^2 = (K_{2\|} + 2K^2_{\perp})/3 \quad (6)$$

K values (Table 2a), for the copper(II) complexes (**2**), (**3**) and(**4**) are indicating for a covalent bond character [34,51]. Kivelson and Neiman noted that, for ionic environment $g_{\|} \geq 2.3$ and for a covalent environment $g_{\|} < 2.3$ [52]. Theoretical work by Smithseems to confirm this view [50]. The g-values reported here (Table 2) show considerable covalent bond character [34]. Also, the in-plane σ-covalency parameter, α^2(Cu) was calculated by

$$\alpha^2 (Cu) = (A_{\|}/0.036)+(g_{\|}-2.002)+3/7(g -2.002)+0.04 \quad (7)$$

The calculated values (Table 2a) suggest a covalent bonding [34,51]. The in-plane and out of-plane π- bonding coefficients β_1^2 and β^2 respectively, are dependent upon the values of ΔE_{xy} and ΔE_{xz} in the following equations [45].

$$\alpha^2\beta^2 = (g_{\perp}- 2.002)\ \Delta E_{xy}/2\lambda_o \quad (8)$$

$$\alpha^2\beta_1^2 = (g_{\|} - 2.002)\ \Delta E_{xz}/8\lambda_o \quad (9)$$

In this work, the complexes (**2**), (**3**) and (**4**) show β_1^2 values 0.88, 0.82 and 0.74 indicating a moderate degree of covalency in the in-plane π-bonding [51,53]. β^2 value forcomplexes (**3**), (**4**) show 1.36 and 1.07 indicating ionic character of the out-of-plane, while β^2 value forcomplex (**2**) is 0.87 indicating a covalent bonding character out-of- plane π-bonding [51,53]. It is possible to calculate approximate orbital populations ford orbitals [29] by

$$A_{\|} = A_{iso} - 2B[1 \pm (7/4)\ \Delta g_{\|}] \quad \Delta g_{\|} = g_{\|} - g_e \quad (10)$$

$$\alpha_{p,d}^{\ 2} = 2B/\ 2B^{\circ} \quad (11)$$

Where A° and 2B° is the calculated dipolar coupling for unit occupancy of d orbital respectively. When the data are analyzed, the components of the Cu hyperfine coupling were considered with all the sign combinations [29]. The only physically meaningful results are found when $A_{\|}$and $A_{\perp}$ were negative. The resulting isotropic coupling constant was negative and the parallel component of the dipolar coupling 2B are negative (-142, -125 and -151 G). These results can only occur for an orbital involving the d_{x2-y2} atomic orbital on copper. The value for 2B is quite normal for copper(Il) complexes [54]. The $|A_{iso}|$ value was relatively small. The 2B value divided by $2B^o$ (The calculated dipolar coupling for unit occupancy of d_{x2-y2} (-235.11 G), using equation (10) suggests all orbital population close to 53-64 % d-orbital spin density, clearly the orbital of the unpaired electron is d_{x2-y2}[55]. Complex (**9**) shows an isotropic spectra with g_{iso}= 2.08.

Table 2a: ESR data for metal (II) complexes

$g_{\perp}$	g_{iso}[a]	$A_{\|}$ (G)	$A_{\perp}$ (G)	A_{iso}[b] (G)	G[c]	ΔE_{xy} (cm^{-1})	ΔE_{xy} (cm^{-1})	$K_{\perp}^2$	$K_{\|}^2$	K^2	K	$g_{\|}/A_{\|}$ (cm^{-1})	α^2	β^2	β_1^2	-2β	$a^2d(\%)$
2.05	2.12	150	15	60	3.28	18018	21277	0.86	0.62	0.78	0.88	149.2	0.70	0.87	0.88	142	61
2.07	2.11	133	10	51	2.85	17857	21505	0.88	0.53	0.76	0.84	173.1	0.65	1.36	0.82	125	53
2.08	2.14	130	10.0	50	3.37	17241	21505	1.01	0.7	0.83	0.94	162.14	0.73	1.07	0.74	151	64
-	2.08	-	-	-	-	-	-	-	-	-	-	-	-	-	-	-	-

[a]g_{iso}= $(2g_{\perp}+ g_{\|})/3$, [b]$A_{iso}=(2A_{\perp}+ A_{\|})/3$, [C]$G = (g_{\|}-2)/ (g_{\perp} -2)$ (12), (13)

Thermal analyses (Differential ThermalAnalysis(DTA) and Thermo Gravimetric Analysis(TGA)): Since the IR spectra indicate the presence of water molecules, thermal analyses (DTA and TGA) were carried out to certain their nature. The thermal curves in the temperature 27-600°range for complexes (**2**), (**3**), (**4**), (**5**) and (**6**) are thermally stable up to 45 °C. Broken of hydrogen bonding occurs as endothermic peak within the temperature 45-50 °C as shown in (Table 2b). Dehydration is characterized by endothermic peak at the temperature 85 °C, corresponding to the loss of hydrated water molecules as in complex (**5**). The elimination of coordinated water molecules occur in 130-150°C range accompanied by endothermic peaks as in complexes (**2**), (**3**), (**4**), (**5**) and (**6**) [60,61]. The TG and DTA thermogramof Cu(II) complex (**2**) showed that, the complexes decomposed in five steps. The first occurred at 50°C with no weight loss as endothermic peak, may be due to break of hydrogen bonding. The second step occurred at 150°C with 5.50% weight loss (Calc. 5.65%) could be due to the elimination of two coordinated H_2O. The TG curve displays another thermal decomposition at 265°C with 9.99% weight loss (Calc. 10.16%), which could be due to the loss of acetate group. The complex shows an exothermic peak observed at 320°C is due its melting point. Finally, exothermic peaks appear at 455, 504, 559, 580 and 595 °C corresponding to oxidative thermal decomposition which proceeds slowly with leaving CuO with 14.71% weight loss (Calc. 14.75%)[62]. The TG and DTA thermogramof Cu(II) Complex (**5**) shows endothermic peak at 85 °C, with 5.03% weight loss (Calc. 5.07%) due to loss of two hydrated water molecule and another endothermic peak at130 °C with 5.26% weight loss (Calc. 5.35%) are assigned to two coordinated water molecules. The endothermic peak observed at 240 and 260°C with 15.04% weight loss (Calc. 15..04%), could be due to the elimination of Sulphate group. Another exothermic peak observed at 350 with no weight loss may be due to its melting point. Finally, the complex shows exothermic peaks at 400, 450, 490, 560 and 590°C with 14.69% weight loss (Calc. 14.70%) corresponding to oxidative thermal decomposition which proceeds slowly with final residue, assigned to CuO[29]. The TG and DTA thermogramof Zn(II) complex (**6**) shows endothermic peak at 50°C, due to break of hydrogen bonding. Another endothermicpeak appeared at 150°C, with 5.40% weight loss (Calc. 5.64%), due to loss of two coordinated water molecules.The endothermic peak observed at 260 with 10.05% weight loss (Calc. 10.13%), could be due to the elimination of acetate group. The complex displayed another exothermic peak at 420°C may be assigned to its melting point. Oxidative thermal decomposition occurs in the 450, 500, 550 and 590°C with exothermic peaks, leaving ZnO with 15.01% weight loss (Calc. 15.04%) [62]. peak appeared at 150°C, with 5.40% weight loss (Calc. 5.64%), due to loss of two coordinated water molecules.The endothermic peak observed at 260 with 10.05% weight loss (Calc. 10.13%), could be due to the elimination of acetate group. The complex displayed another exothermic peak at 420°C may be assigned to its melting point. Oxidative thermal decomposition occurs in the 450, 500, 550 and 590°C with exothermic peaks, leaving ZnO with 15.01% weight loss (Calc. 15.04%) [62].

C**hemotherapeutic studies:** The biological activity of the ligand **(1)** and its metal complexes **(2)**, **(3)**, **(4)**, **(5)**, **(9)** and **(10)** were evaluated against HEPG-2 cell line.In this study, we try to know the chemotherapeutic activity of the tested complexes by comparing them with the standard drug (Vinblastine Sulfate). The treatment of the different complexes in DMSO showed similar effect in the tumoral cell line used as it was previously reported[63]. The solvent dimethyl sulphoxide (DMSO) shows no effect in cell growth. The ligand **(1)** shows a weak inhibition effect at ranges of concentrations used, however, the complexes showed better effect against HEPG-2 cell line. The obtained data indicate the surviving fraction ratio against HEPG-2 tumor cell line increasing with the decrease of the concentration in the range of the tested concentrations. Also, the Cu(II) complex **(2)** shows the highest potency of inhibition at 500 µg/ml against HEPG-2 cell line, compared with the standard drug [51].Cytotoxicity results indicated that the tested complexes **(2)**

and **(3)** (IC_{50} = 0.95–0.98 µg/ml) demonstrated potent cytotoxicity against HepG2 cancer cells Figures6-8. Copper complex **(3)** showed the highest cytotoxicity effect against HEPG-2 cell line with IC_{50} value of 0.95 µg/ml, followed by copper complex **(2)** with IC_{50} value 0.98 µg/ml. The cytotoxicity of the copper complexes **(2), (3)** and **(4)** are more active than standard drugs used. This can be explained as Cu(II) ion binds to DNA. It seems that, changing the anion and the nature of the metal ion has effect on the biological behavior, due to alter binding ability of DNA binding, so testing of different complexes is very interesting from this point of view. Chemotherapeutic activity of the complexes may be attributed to the central metal atom which was explained by Tweedy's chelation theory [63,64]. Also, the positive charge of the metal increases the acidity of coordinated ligand that bears protons, leading to stronger hydrogen bonds which enhance the biological activity [65,66]. Moreover, Gaetke and Chow had reported that, metal has been suggested to facilitate oxidated tissue injury through a free-radical mediated pathway analogous to the Fenton reaction [66]. By applying the ESR-trapping technique, evidence for metal - mediated hydroxyl radical formation in vivo has been obtained [48]. ROS are produced through a Fenton-type reaction as follows:

$$LM(II) + H_2O_2 \rightarrow LM(I) + .OOH + H^+$$

$$LM(I) + H_2O_2 \rightarrow LM(II) + .OH + OH^-$$

Where L, organic ligand

Table 2b: Thermal analyses for metal (II) complexes

NO.	Molecular formula	Temp. (°C)	DTA (peak)		TGA (Wt.loss %)		Assignments
			Endo	Exo	Calcd.	Found	
(2)	[(HL)Cu(CH3COO)(H2O)2]	50	Endo	-	-	-	Broken of H-bonding
		150	Endo	-	5.65	5.5	Loss of (2H2O) coordinated water molecules
		265	Endo	-	10.16	9.99	Loss of acetate group
		320	-	Exo	-	-	Melting point
		455,504,559,580,595	-	Exo	14.75	14.71	Decomposition process with the formation of CuO
(3)	[(L)Cu(CH3COO)(H2O)2]2	49	endo	-	-	-	Broken of H-bonding
		140	endo	-	4.89	4.83	Loss of (2H2O) coordinated water molecules
		250,270	endo	-	16.11	16.02	Loss of two acetate groups
		363	-	exo	-	-	Melting point
		405,450,485,565,580	-	exo	25.02	24.99	Decomposition process with the formation of 2CuO
(4)	[(HL)(Cu)Cl(H2O)2]	50	endo	-	-	-	Broken of H-bonding
		130	endo	-	5.88	5.84	Loss of (2H2O) coordinated water molecules
		260	endo	-	6.14	6.13	Loss of Cl ion
		325	-	exo	-	-	Melting point
		350,380,450,500,590	-	exo	14.70	14.68	Decomposition process with the formation of CuO
(5)	[(H2L)Cu(SO4)(H2O)2].2H2O	45	endo	-	-	-	Broken of H-bonding
		85	endo	-	5.07	5.03	Loss of (2H2O) hydrated water molecules
		130	endo	-	5.35	5.26	Loss of (2H2O) Coordinated water molecules
		240,260	endo	-	15.07	15.04	Loss of SO4 group
		350	-	exo	-	-	Melting point
		400,450,490,560,590		exo	14.70	14.69	Decomposition process with the formation of CuO
(6)	[(HL)Zn(CH3COO)(H2O)2]	50	endo	-	-	-	Broken of H-bonding
		150	endo	-	5.64	5.40	Loss of (2H2O) coordinated water molecules
		260	endo		10.13	10.05	Loss of acetate group
		420	-	exo	-	-	Melting point
		450,500,550,590	-	exo	15.04	15.01	Decomposition process with the formation of ZnO

Also, metal could act as a double-edged sword by inducing DNA damage and also by inhibiting their repair [67]. The OH radicals react with DNA sugars and bases and the most significant and well-characterized of the OH reactions is hydrogen atom abstraction from the C4 on the deoxyribose unit to yield sugar radicals with subsequent β-elimination (Scheme 2). By this mechanism strand break occurs as well as the release of the free bases. Another form of attack on the DNA bases is by solvated electrons, probably via a similar reaction to those discussed below for the direct effects of radiation on DNA [68]. In the ranges of concentrations used, the chemotherapeutic effect against HEPG-2 cell line are depicted in (Table 4), although, the complexes have the same anions, the variable activity of the complexes may be used to oxidation – reduction potentials. The cytotoxic effect of standard drugs and metal complexes in the ranges of concentrations used against human HEPG-2 cell lineare shown in Figures 6-8.

Table 3: Order of cytotoxic effect of the studied complexes against HEPG-2 and MCF-7 cell line

concentration	**Order of cytotoxic effect of studied complex**
	(HEPG-2 cell line)
500 µg/ml	(2)>(3)>(4)>std.>(10)>(1).>(8)> (9)
125µg/ml	(2)>(3)>(4) >std.>(8)>(10).>(1)> (9)
31.25µg/ml	Std.>(2)>(3) >(4)>(10)>(1).>(8)> (9)
7.8µg/ml	(3)>(2)>(4) >std.>(8)>(10).>(1)> (9)
2.0µg/ml	(2)>(3)>(4) >(8).>std.>(10).>(1)> (9)
1.0µg/ml	(3)>(2)>std.>(4)>(8)>(10).>(1)> (9)

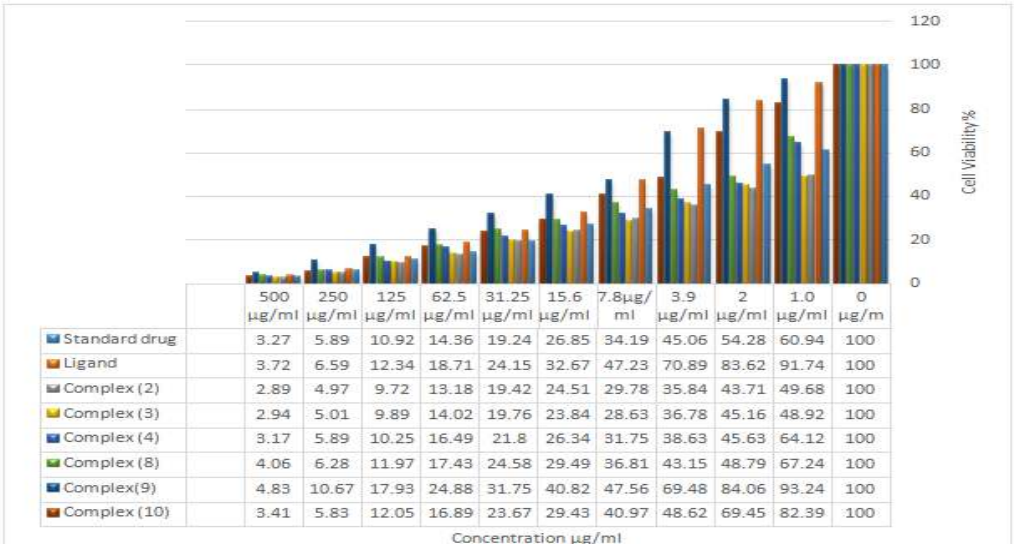

	500 µg/ml	250 µg/ml	125 µg/ml	62.5 µg/ml	31.25 µg/ml	15.6 µg/ml	7.8µg/ml	3.9 µg/ml	2 µg/ml	1.0 µg/ml	0 µg/m
Standard drug	3.27	5.89	10.92	14.36	19.24	26.85	34.19	45.06	54.28	60.94	100
Ligand	3.72	6.59	12.34	18.71	24.15	32.67	47.23	70.89	83.62	91.74	100
Complex (2)	2.89	4.97	9.72	13.18	19.42	24.51	29.78	35.84	43.71	49.68	100
Complex (3)	2.94	5.01	9.89	14.02	19.76	23.84	28.63	36.78	45.16	48.92	100
Complex (4)	3.17	5.89	10.25	16.49	21.8	26.34	31.75	38.63	45.63	64.12	100
Complex (8)	4.06	6.28	11.97	17.43	24.58	29.49	36.81	43.15	48.79	67.24	100
Complex(9)	4.83	10.67	17.93	24.88	31.75	40.82	47.56	69.48	84.06	93.24	100
Complex (10)	3.41	5.83	12.05	16.89	23.67	29.43	40.97	48.62	69.45	82.39	100

Fig.6 : Evaluation of cytotoxicity of metal complexes Against human hepatic HEPG-2 Cell Line

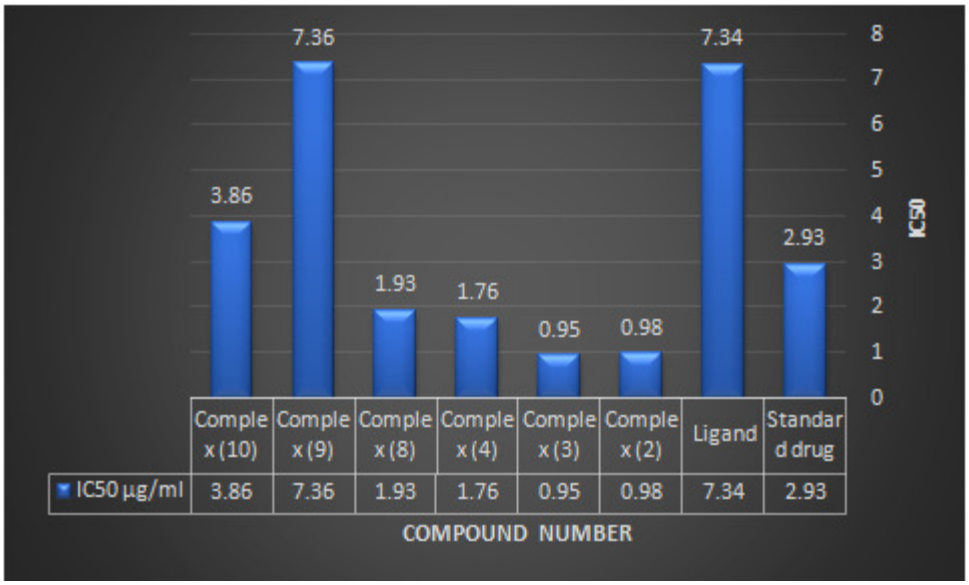

Fig.7: IC_{50} values of the ligand, H_2L (1) and its metal complexes against human hepatic HEPG-2 cell lines.

Moreover, Gaetke and Chow had reported that, metal has been suggested to facilitate oxidated tissue injury through a free-radical mediated pathway analogous to the Fenton reaction [66]. By applying the ESR-trapping technique, evidence for metal - mediated hydroxyl radical formation in vivo has been obtained [48]. ROS are produced through a Fenton-type reaction as follows:

$$LM(II) + H_2O_2 \rightarrow LM(I) + .OOH + H^+$$

$$LM(I) + H_2O_2 \rightarrow LM(II) + .OH + OH^-$$

Where L, organic ligand.Also, metal could act as a double-edged sword by inducing DNA damage and also by inhibiting their repair [67]. The OH radicals react with DNA sugars and bases and the most significant and well-characterized of the OH reactions is hydrogen atom abstraction from the C4 on the deoxyribose unit to yield sugar radicals with subsequent β-elimination (Scheme 2). By this mechanism strand break occurs as well as the release of the free bases. Another form of attack on the DNA bases is by solvated electrons, probably via a similar reaction to those discussed below for the direct effects of radiation on DNA [68].

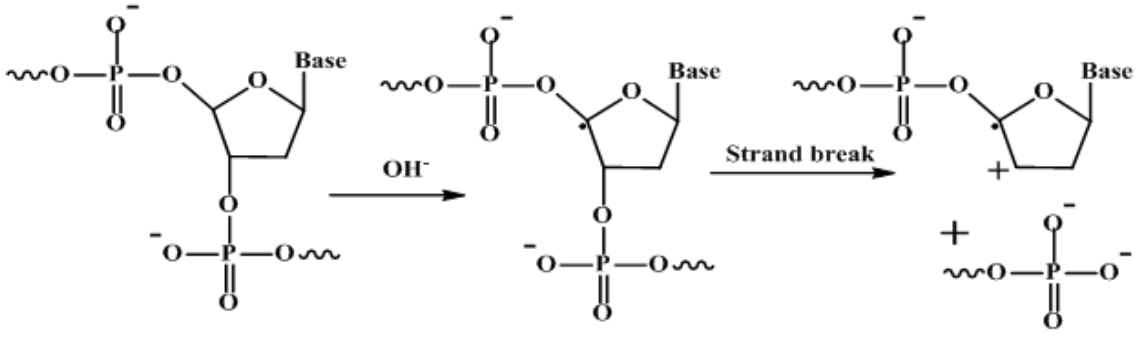

Scheme 2: Suggested mechanism for OH radicals attack on DNA sugars and bases

In the ranges of concentrations used, the chemotherapeutic effect against HEPG-2 cell line are depicted in (Table 4), although, the complexes have the same anions, the variable activity of the complexes may be used to oxidation – reduction potentials. The cytotoxic effect of standard drugs and metal complexes in the ranges of concentrations used against human HEPG-2 cell line are shown in Figures 6-8

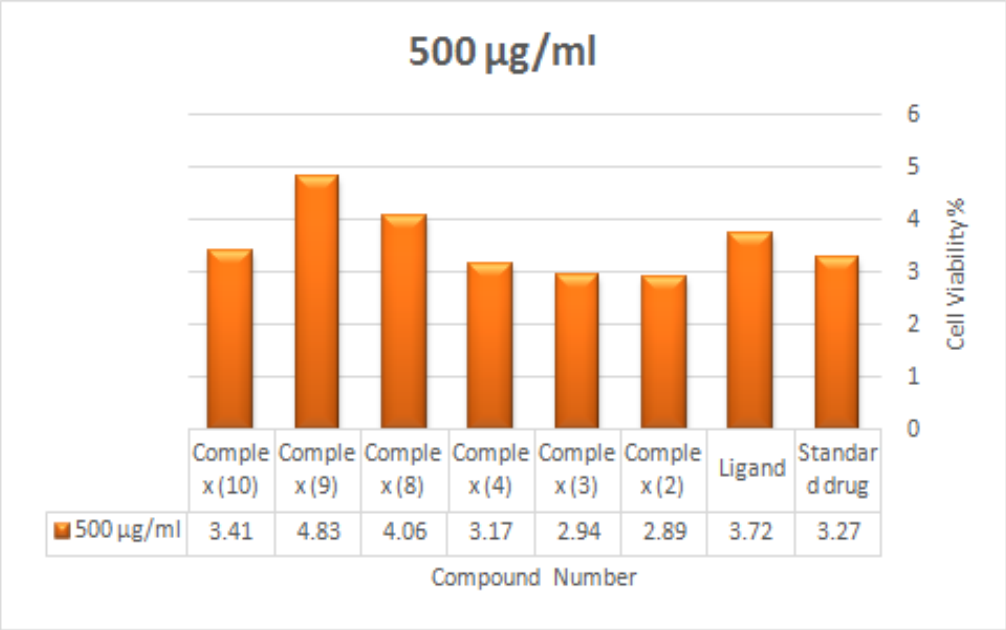

Fig.8: Evaluation of cytotoxicity of metal complexes Against human hepatic HEPG-2 Cell Line at 500 µg/ml

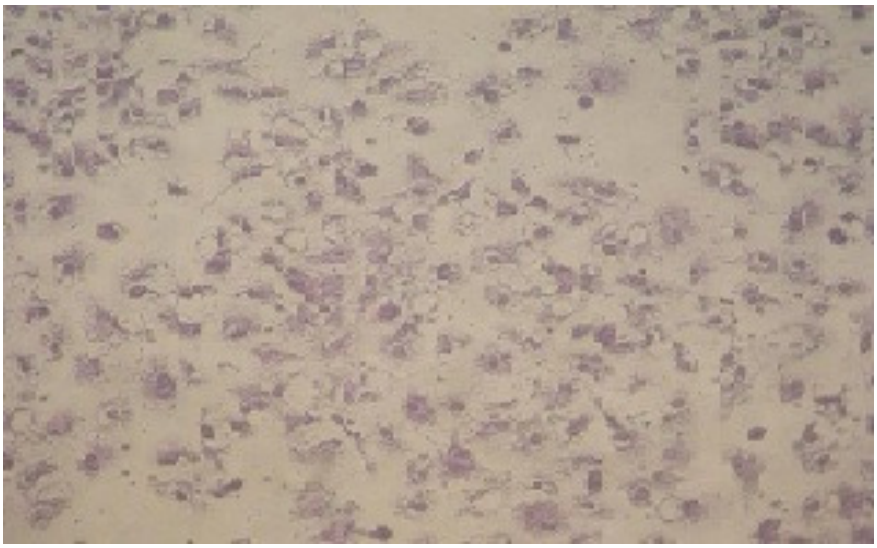

Fig. 9: Histogram showed HepG cells treated with standard drug at 500 ug

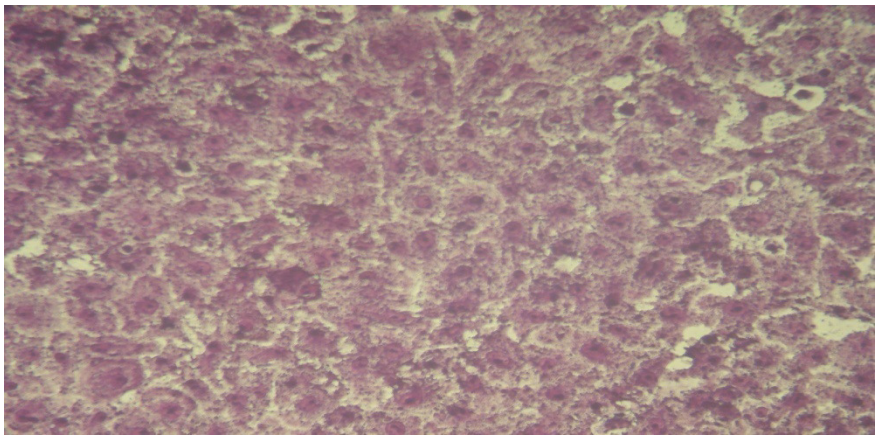

Fig. 10: Histogram showed HepG cells treated with complex (2) at 0.5ug

Fig. 11: Histogram showed HepG cells treated with complex (2) at 500 ug

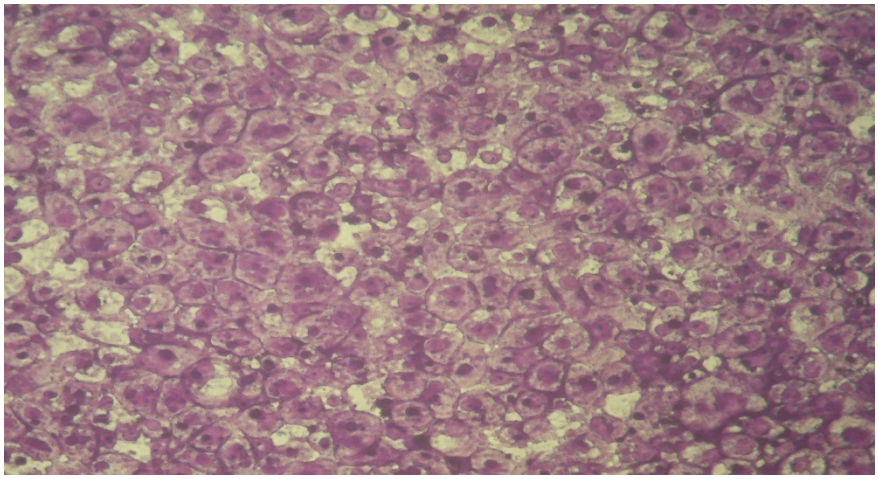

Fig. 12: Histogram showed HepG cells treated with complex (3) at 0.5ug

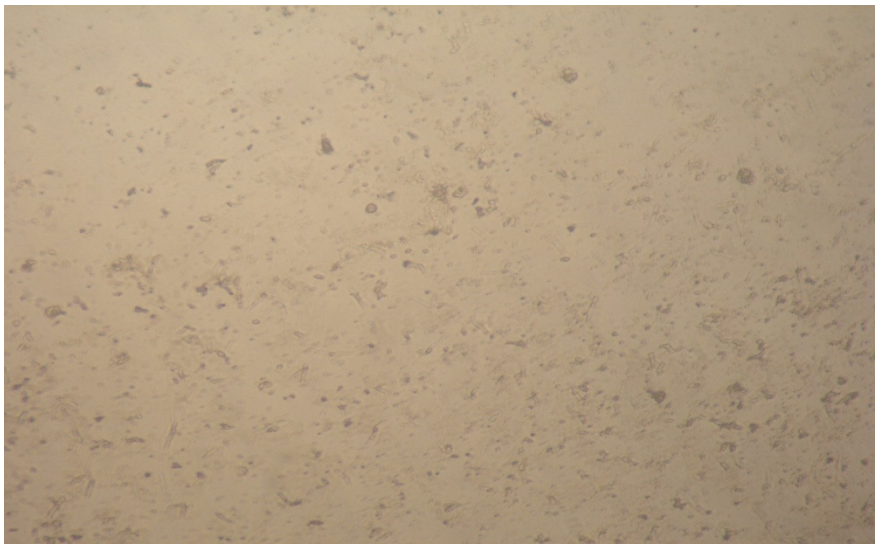

Fig. 13: Histogram showed HepG cells treated with complex (3) at 500 ug

5. CONCLUSION

Novel Schiff base ligand, N^1,N^2-bis(2-aminophenyl)oxalamide and its copper(II), manganese(II), zinc(II) and silver(I) metal complexes were synthesized. The analytical and physicochemical data confirmed the composition and structure of the newly obtained compounds. The ESR spectra of solid Cu (II) complexes **(2-4)** show axial type indicating a $d_{(X^2-y^2)}$ ground state with significant covalent bond character. The complexes adopted distorted octahedral geometry around the metal ion. The ligand and its copper (II) complexes showed a high potential cytotoxic activity against growth human liver cancer HepG2 tumor compared to (Vinblastine Sulfate) standard drug. The tested complexes were found to be more active than the free ligand. This indicates enhancing of antitumor activity upon coordination. Copper complex **(2)** showed the highest cytotoxic activity against, HEPG-2 cell line with IC_{50} 0.98 $\mu g/ml$. These compounds are promising candidates as anticancer agents because of their high cytotoxic activities.

ACKNOWLEDGEMENT

The authors express their sincere gratitude to Academy of Scientific Research and Technology (Cairo, Egypt) for their financial support for the research and their great thanks to Nourhan Mohammed Ibrahim Ebada (Department of Physics, Faculty of Education, Sadat University, Egypt) for supporting this research to reach this good image.

REFERENCES

[1] LEWIS, D. F. 1996. Guide to cytochromes: structure and function, CRC Press.
[2] DE BONO, J. S., LOGOTHETIS, C. J., MOLINA, A., FIZAZI, K., NORTH, S., CHU, L., CHI, K. N., JONES, R. J., GOODMAN JR, O. B. & SAAD, F. 2011. Abiraterone and increased survival in metastatic prostate cancer. New England Journal of Medicine, 364, 1995-2005.
[3] XIAO, Y., BI, C., FAN, Y., LIU, S., ZHANG, X., ZHANG, D., WANG, Y. & ZHU, R. 2009. Synthesis, characterization and bioactivity of Schiff base copper (II) complexes derived from L-glutamine and L-asparagine. Journal of Coordination Chemistry, 62, 3029-3039.
[4] SOLOMON, E. I. & LOWERY, M. D. 1993. Electronic structure contributions to function in bioinorganic chemistry. Science, 259, 1575-1582.

[5] ANACONA, J., NORIEGA, N. & CAMUS, J. 2015. Synthesis, characterization and antibacterial activity of a tridentate Schiff base derived from cephalothin and sulfadiazine, and its transition metal complexes. Spectrochimica Acta Part A: Molecular and Biomolecular Spectroscopy, 137, 16-22.
[6] SHOHAYEB, S. M., MOHAMED, R. G., MOUSTAFA, H. & EL-MEDANI, S. M. 2016. Synthesis, spectroscopic, DFT calculations and biological activity studies of ruthenium carbonyl complexes with 2-picolinic acid and a secondary ligand. Journal of Molecular Structure, 1119, 442-450.
[7] GERDEMANN, C., EICKEN, C. & KREBS, B. 2002. The crystal structure of catechol oxidase: new insight into the function of type-3 copper proteins. Accounts of chemical research, 35, 183-191.
[8] BRATSOS, I., GIANFERRARA, T., ALESSIO, E., HARTINGER, C. G., JAKUPEC, M. A. & KEPPLER, B. K. 2011. Ruthenium and Other Non-Platinum Anticancer Compounds. Bioinorganic Medicinal Chemistry, 151-174.
[9] GIELEN, M. & TIEKINK, E. R. 2005. Metallotherapeutic drugs and metal-based diagnostic agents: the use of metals in medicine, John Wiley & Sons.
[10] VOGEL, A. I. & SVEHLA, G. 1979. Vogel's macro and semimicro qualitative inorganic analysis.
[11] WELCHER, F. J. 1958. The analytical Uses of ethylenediamine tetraacetic acid by Frank Johnson Welcher.
[12] VOGEL, A. & BASSETT, J. 1978. Vogel's textbook of quantitative inorganic analysis, including elementary instrumental analysis 4th. Edn. London and New York.
[13] LEWIS, J. & WILKINS, R. G. 1960. Modern coordination chemistry.
[14] VICHAI, V. & KIRTIKARA, K. 2006. Sulforhodamine B colorimetric assay for cytotoxicity screening. Nature protocols, 1, 1112-1116.
[15] EL-TABL, A. S., MOHAMED ABD EL-WAHEED, M., WAHBA, M. A. & ABD EL-HALIM ABOU EL-FADL, N. 2015. Synthesis, characterization, and anticancer activity of new metal complexes derived from 2-hydroxy-3-(hydroxyimino)-4-oxopentan-2-ylidene) benzohydrazide. Bioinorganic chemistry and applications, 2015.
[16] NICODEMO, A., ARAUJO, M., RUIZ, A. & GALES, A. C. 2004. In vitro susceptibility of Stenotrophomonas maltophilia isolates: comparison of disc diffusion, Etest and agar dilution methods. Journal of Antimicrobial Chemotherapy, 53, 604-608.
[17] ABDOU, S., ABD-EL WAHED, M. M., WAHBA, M. A., SHAKDOFA, M. M. & ABU-SETTA, M. H. 2015. Journal of Chemical, Biological and Physical Sciences. 5, 3697-3720.
[18] COLLEE, J. 1989. Mackie and McCartney practical medical microbiology.
[19] YU, Y.-Y., XIAN, H.-D., LIU, J.-F. & ZHAO, G.-L. 2009. Synthesis, characterization, crystal structure and antibacterial activities of transition metal (II) complexes of the Schiff base 2-[(4-methylphenylimino) methyl]-6-methoxyphenol. Molecules, 14, 1747-1754.
[20] MISHRA, D., NASKAR, S., DREW, M. G. & CHATTOPADHYAY, S. K. 2006. Synthesis, spectroscopic and redox properties of some ruthenium (II) thiosemicarbazone complexes: structural description of four of these complexes. Inorganica Chimica Acta, 359, 585-592.
[21] EL-TABL, A. S., ABD-EL WAHED, M. M., WAHBA, M. A., FARID, R. W. & HASHIM, S. M. F. 2015. Synthesis, Characterization and Antimicrobial activity of New Binary Metal Complexes Derived from Amino Sulfo-Naphthalene Ligand. Journal of Chemical, Biological and Physical Sciences (JCBPS), 5, 3629.
[22] MAURYA, M. R., KHURANA, S., SCHULZKE, C. & REHDER, D. 2001. Dioxo-and Oxovanadium (V) Complexes of Biomimetic Hydrazone ONO Donor Ligands: Synthesis, Characterisation, and Reactivity. European Journal of Inorganic Chemistry, 2001, 779-788.
[23] MAURYA, M. R., AGARWAL, S., BADER, C. & REHDER, D. 2005. Dioxovanadium (V) Complexes of ONO Donor Ligands Derived from Pyridoxal and Hydrazides: Models of Vanadate-Dependent Haloperoxidases. European Journal of Inorganic Chemistry, 2005, 147-157.
[24] EL-TABL, A. S., EL-SAIED, F. A. & AL-HAKIMI, A. N. 2007. Synthesis, spectroscopic investigation and biological activity of metal complexes with ONO trifunctionalalized hydrazone ligand. Transition Metal Chemistry, 32, 689-701.
[25] EL-TABL, A. S., SHAKDOFA, M. M. & EL-SEIDY, A. 2011. Synthesis, Characterization and ESR Studies of New Copper (II) Complexes of Vicinal Oxime Ligands. Journal of the Korean Chemical Society, 55, 603-611.
[26] ATEŞ, D., GULCAN, M., GUMUŞ, S., ŞEKERCI, M., ÖZDEMIR, S., ŞAHIN, E. & ÇOLAK, N. 2017. Synthesis of bis (thiosemicarbazone) derivatives: Definition, crystal structure, biological potential and computational analysis. Phosphorus, Sulfur, and Silicon and the Related Elements, 1-9.
[27] EL-TABL, A., KASHAR, T., EL-BAHNASAWY, R. & IBRAHIM, A. E.-M. 1999. Sythesis and characterization of novel copper (II) complexes of dehydroacetic acid thiosemicarrbazone. Polish Journal of Chemistry, 73, 245-254.
[28] EL-TABL, A. S. 2002. Synthesis and physico-chemical studies on cobalt (II), nickel (II) and copper (II) complexes of benzidine diacetyloxime. Transition Metal Chemistry, 27, 166-170.

[29] EL-TABL, A. S., EL-WAHED, M. M. A. & REZK, A. M. S. M. 2014. Cytotoxic behavior and spectroscopic characterization of metal complexes of ethylacetoacetate bis (thiosemicarbazone) ligand. Spectrochimica Acta Part A: Molecular and Biomolecular Spectroscopy, 117, 772-788.
[30] KUSKA, H., ROGERS, M. & MARTELL, A. 1971. Coordination chemistry. Van Nostrand Reinhold Co., New York.
[31] FOUDA, M. F., ABD-ELZAHER, M. M., SHAKDOFA, M. M., EL-SAIED, F. A., AYAD, M. I. & EL TABL, A. S. 2008. Synthesis and characterization of a hydrazone ligand containing antipyrine and its transition metal complexes. Journal of Coordination Chemistry, 61, 1983-1996.
[32] FADDA, A. A. & ELATTAR, K. M. 2016. Reactivity of dehydroacetic acid in organic synthesis. Synthetic Communications, 46, 1-30.
[33] GUDASI, K. B., PATIL, M. S., VADAVI, R. S., SHENOY, R. V., PATIL, S. A. & NETHAJI, M. 2006. X-ray crystal structure of the N-(2-hydroxy-1-naphthalidene) phenylglycine Schiff base. Synthesis and characterization of its transition metal complexes. Transition Metal Chemistry, 31, 580-585.
[34] AL-HAKIMI, A. N., SHAKDOFA, M. M., EL-SEIDY, A. & EL-TABL, A. S. 2011. Synthesis, Spectroscopic, and Biological Studies of Chromium (III), Manganese (II), Iron (III), Cobalt (II), Nickel (II), Copper (II), Ruthenium (III), and Zirconyl (II) Complexes of N 1, N 2-Bis (3-((3-hydroxynaphthalen-2-yl) methylene-amino) propyl) phthalamide. Journal of the Korean Chemical Society, 55, 418-429.
[35] EL-TABL, A. S. 1997. Novel N, N-diacetyloximo-1, 3-phenylenediamine copper (II) complexes. Transition Metal Chemistry, 22, 400-405.
[36] RAMADAN, A. E.-M. M., SAWODNY, W., EL-BARADIE, H. Y. & GABER, M. 1997. Synthesis and characterization of nickel (II) complexes with symmetrical tetradentate N 2 O 2 naphthaldimine ligands. Their application as catalysts for the hydrogenation of cyclohexene. Transition Metal Chemistry, 22, 211-215.
[37] EL-TABL, A. S. & EL-ENEIN, S. A. 2004. Reactivity of the new potentially binucleating ligand, 2-(acetichydrazido-N-methylidene-α-naphthol)-benzothiazol, towards manganese (II), nickel (II), cobalt (II), copper (II) and zinc (II) salts. Journal of Coordination Chemistry, 57, 281-294.
[38] SALLAM, S. A., ORABI, A. S., EL-SHETARY, B. A. & LENTZ, A. 2002. Copper, nickel and cobalt complexes of Schiff-bases derived from β-diketones. Transition Metal Chemistry, 27, 447-453.
[39] SINGH, U., BUKHARI, M. N., ANAYUTULLAH, S., ALAM, H., MANZOOR, N. & HASHMI, A. A. 2016. Synthesis, Characterization and Biological Evaluation of Metal Complexes with Water-Soluble Macromolecular Dendritic Ligand. Pharmaceutical Chemistry Journal, 49, 868-877.
[40] EL-TABL, A. S., EL-SAIED, F. A. & AL-HAKIMI, A. N. 2008. Spectroscopic characterization and biological activity of metal complexes with an ONO trifunctionalized hydrazone ligand. Journal of Coordination Chemistry, 61, 2380-2401.
[41] SINGH, N. K. & SINGH, S. B. 2001. Complexes of 1-isonicotinoyl-4-benzoyl-3-thiosemicarbazide with manganese (II), iron (III), chromium (III), cobalt (II), nickel (II), copper (II) and zinc (II). Transition Metal Chemistry, 26, 487-495.
[42] PARIHARI, R., PATEL, R. & PATEL, R. 2000. Synthesis and characterization of metal complexes of manganese-, cobalt-and zinc (II) with Schiff base and some neutral ligand. Journal of The Indian Chemical Society, 77, 339-340.
[43] THAKKAR, N. & BOOTWALA, S. 1995. Synthesis and characterization of binuclear metal complexes derived from some isonitrosoacetophenones and benzidine.
[44] CHIUMIA, G. C., PHILLIPS, D. J. & RAE, A. D. 1995. N-Oxide-bridged complexes of cobalt (II) and nickel (II) with 2-acetylpyridine 1-oxide oxime (pro). X-ray crystal structure of the dimeric complex [Co (pxo)(CH3OH) Cl2] 2. Inorganica Chimica Acta, 238, 197-201.
[45] EL-BORAEY, H. 2003. Supramolecular copper (II) complexes with tetradentate ketoenamine ligands. Polish Journal of Chemistry, 77, 1759-1775.
[46] EL-TABL, A. S. 1997. An esr study of copper (II) complexes of N-hydroxyalkylsalicylideneimines. Transition Metal Chemistry, 23, 63-65.
[47] ROSU, T., PAHONTU, E., PASCULESCU, S., GEORGESCU, R., STANICA, N., CURAJ, A., POPESCU, A. & LEABU, M. 2010. Synthesis, characterization antibacterial and antiproliferative activity of novel Cu (II) and Pd (II) complexes with 2-hydroxy-8-R-tricyclo [7.3. 1.0. 2, 7] tridecane-13-one thiosemicarbazone. European journal of medicinal chemistry, 45, 1627-1634.
[48] NIKLES, D., POWERS, M. & URBACH, F. 1983. Copper (II) complexes with tetradentate bis (pyridyl)-dithioether and bis (pyridyl)-diamine ligands. Effect of thio ether donors on the electronic absorption spectra, redox behavior, and EPR parameters of copper (II) complexes. Inorganic Chemistry, 22, 3210-3217.
[49] TIITTA, M. & NIINISTOU, L. 1997. Volatile Metal β-Diketonates: ALE and CVD precursors for electroluminescent device thin films. Chemical Vapor Deposition, 3, 167-182.
[50] CARL, P. J. & LARSEN, S. C. 1999. Variable-temperature electron paramagnetic resonance studies of copper-exchanged zeolites. Journal of catalysis, 182, 208-218.

[51] EL-TABL, A. S., SHAKDOFA, M. M. & SHAKDOFA, A. M. 2013. Metal complexes of N'-(2-hydroxy-5-phenyldiazenyl) benzylideneisonicotinohydrazide: Synthesis, spectroscopic characterization and antimicrobial activity. Journal of the Serbian Chemical Society, 78, 39-55.

[52] KIVELSON, D. & NEIMAN, R. 1961. ESR studies on the bonding in copper complexes. The Journal of Chemical Physics, 35, 149-155.

[53] BHADBHADE, M. & SRINIVAS, D. 1993. Erratum to document cited in CA119 (26): 285036b. Inorg. Chem, 32, 2458.

[54] MUNIYANDI, V., PRAVIN, N., SUBBARAJ, P. & RAMAN, N. 2016. Persistent DNA binding, cleavage performance and eco-friendly catalytic nature of novel complexes having 2-aminobenzophenone precursor. Journal of Photochemistry and Photobiology B: Biology, 156, 11-21.

[55] SHAKDOFA, M. M., AL-HAKIMI, A. N., ELSAIED, F. A., ALASBAHI, S. O. & ALKWLINI, A. M. 2017. Synthesis, characterization and bioactivity [Zn. sup. 2+],[Cu. sup. 2+],[Ni. sup. 2+],[Co. sup. 2+],[Mn. sup. 2+],[Fe. sup. 3+],[Ru. sup. 3+], V [O. sup. 2+] and U [O. sub. 2. sup. 2+] complexes of 2-hydroxy-5-((4-nitrophenyl) diazenyl) benzylidene)-2-(p-tolylamino) acetohydrazide. Bulletin of the Chemical Society of Ethiopia, 31, 75-92.

[56] NATARAJAN, C., SHANTHI, P., ATHAPPAN, P. & MURUGESAN, R. 1992. Synthesis and spectral studies of cobalt (II), nickel (II) and copper (II) complexes of 1-(2-hydroxy-1-naphthyl)-3-(4-X-phenyl)-2-propen-1-ones and their pyridine adducts. Transition Metal Chemistry, 17, 39-45.

[57] BERTRAND, J., BLACK, T., ELLER, P. G., HELM, F. & MAHMOOD, R. 1976. Polynuclear complexes with hydrogen-bonded bridges. Dinuclear complex of N, N'-bis (2-hydroxyethyl)-2, 4-pentanediimine with copper (II). Inorganic Chemistry, 15, 2965-2970.

[58] SHIEH, S.-J., CHEA, C.-M. & PENG, S.-M. 1992. A colorless Cu (II) complex of CuO 6 with a compressed tetragonal octahedron. Inorganica Chimica Acta, 192, 151-152.

[59] EL-TABL, A. 1997. Synthesis and spectral studies on mononuclear copper (II) complexes of isonitrosoacetylacetone ligand. Polish Journal of Chemistry, 71, 1213-1222.

[60] EL-TABL, A. S. & IMAM, S. M. 1997. New copper (II) complexes produced by the template reaction of acetoacetic-2-pyridylamide and amino-aliphatic alcohols. Transition Metal Chemistry, 22, 259-262.

[61] EL-TABL, A. S., ABD-EL WAHED, M. M., WAHBA, M. A., SHAKDOFA, M. &GAFER, A. 2016. Bimetallic Transition Metal Complexes of 2, 3-Dihydroxy-N', N'4-bis ((2-Hydroxynaphthalen-1-yl) Methylene) Succinohydrazide Ligand as a New Class of Bioactive Compounds; Synthesis, Characterization and Cytotoxic Evaluation. Indian Journal of Advances in Chemical Science, 4, 114-29.

[62] EL-TABL, A. & ABOU-SEKKINA, M. 1999. Preparation and thermophysical properties of new cobalt (II), nickel (II) and copper (II) complexes. Polish Journal of Chemistry, 73, 1937-1945.

[63] ILLáN-CABEZA, N. A., GARCíA-GARCíA, A. R., MORENO-CARRETERO, M. N., MARTíNEZ-MARTOS, J. M. & RAMíREZ-EXPóSITO, M. J. 2005. Synthesis, characterization and antiproliferative behavior of tricarbonyl complexes of rhenium (I) with some 6-amino-5-nitrosouracil derivatives: Crystal structure of fac-[ReCl (CO) 3 (DANU-N 5, O 4)](DANU= 6-amino-1, 3-dimethyl-5-nitrosouracil). Journal of inorganic biochemistry, 99, 1637-1645.

[64] HALL, I. H., LEE, C. C., IBRAHIM, G., KHAN, M. A. & BOUET, G. M. 1997. Cytotoxicity of metallic complexes of furan oximes in murine and human tissue cultured cell lines. Applied organometallic chemistry, 11, 565-575.

[65] FENG, G., MAREQUE-RIVAS, J. C., TORRES MARTIN DE ROSALES, R. & WILLIAMS, N. H. 2005. A highly reactive mononuclear Zn (II) complex for phosphodiester cleavage. Journal of the American Chemical Society, 127, 13470-13471.

[66] DALLE, K. E. & MEYER, F. 2015. Modelling Binuclear Metallobiosites: Insights from Pyrazole-Supported Biomimetic and Bioinspired Complexes. European Journal of Inorganic Chemistry, 2015, 3391-3405.

[67] ROUZER, C. 2010. Metals and DNA repair. Chemical Research in Toxicology, 23, 1517-1518.

[68] GHONEIM, M., EL-SONBATI, A., EL-BINDARY, A., DIAB, M. & SERAG, L. 2015. Polymer complexes. LX. Supramolecular coordination and structures of N (4-(acrylamido)-2-hydroxybenzoic acid) polymer complexes. Spectrochimica Acta Part A: Molecular and Biomolecular Spectroscopy, 140, 111-131.

[69] ISPIR, E., TOROĞLU, S. & KAYRALDıZ, A. 2008. Syntheses, characterization, antimicrobial and genotoxic activities of new Schiff bases and their complexes. Transition Metal Chemistry, 33, 953-960.